

Distribution function of the dark matter

N. Wyn Evans^{1,*} and Jin H. An^{1,2,†}

¹*Institute of Astronomy, University of Cambridge, Madingley Road, Cambridge, CB3 0HA, United Kingdom*

²*MIT Kavli Institute for Astrophysics & Space Research,
Massachusetts Institute of Technology, 77 Massachusetts Avenue, Cambridge, MA 02139, USA*

There is good evidence from N-body simulations that the velocity distribution in the outer parts of halos is radially anisotropic, with the kinetic energy in the radial direction roughly equal to the sum of that in the two tangential directions. We provide a simple algorithm to generate such cosmologically important distribution functions. Introducing $r_E(E)$, the radius of the largest orbit of a particle with energy E , we show how to write down almost trivially a distribution function of the form $f(E, L) = L^{-1}g(r_E)$ for any spherical model – including the ‘universal’ halo density law (Navarro-Frenk-White profile). We in addition give the generic form of the distribution function for any model with a local density power-law index α and anisotropy parameter β and provide limiting forms appropriate for the central parts and envelopes of dark matter halos. From those, we argue that, regardless of the anisotropy, the density falloff at large radii must evolve to $\rho \sim r^{-4}$ or steeper ultimately.

PACS numbers: 95.35.+d, 98.62.Gq

I. INTRODUCTION

N-body experiments now can reliably follow the collapse and violent relaxation of dark matter halos from initial conditions. This has led to the discovery of regularities in the phase space distribution of dark matter [e.g., 1], even though the final state is not completely independent of initial conditions. This is important because it suggests that there is a generic functional form for the distribution function (DF) that describes the physics of violent relaxation, albeit with some cosmic scatter [2].

For example, Hansen and Moore [3, see also 4] have found that the density power index is correlated with the anisotropy parameter $\beta = 1 - \langle v_T^2 \rangle / (2\langle v_r^2 \rangle)$ [5]. Here, $\langle v_r^2 \rangle$ and $\langle v_T^2 \rangle$ are the radial and the tangential velocity second moments. For a wide range of cosmological simulations, they demonstrate that the dark matter follows the equation of state $\beta \approx 1 - 1.15(1 - \alpha/6)$ where α is the density power index (i.e., $\rho \sim r^{-\alpha}$). In the very center, dark matter halos are roughly isotropic ($\beta \approx 0$) with $\alpha \approx 1$. In the outer parts, violent relaxation produces a density profile that asymptotically becomes $\rho \sim r^{-4}$ [6] or $\rho \sim r^{-3}$ [7], for which the anisotropy parameter $\beta \approx 0.5$ accordingly.

If violent relaxation proceeded to completion, then equipartition would enforce equal kinetic energy in each direction and the velocity distribution would be isotropic [8]. This appears to be the case only at the centers of numerical simulations. Particles with large apocenters respond only weakly to the fluctuating gravitational field. Throughout most of the halo, this gives rise to an end point for which the kinetic energy in the radial direction is roughly equal to the sum of that in the two tangential directions. This seems to be supported not only by the numerical simulations but also by the observation of stars in elliptical galaxies [9], whose kinematics is also governed by the collisionless Boltzmann equation with the gravi-

tational potential. The purpose of this paper is to give the DF of the dark matter which has this property.

There has been much work on isotropic DFs [see 5] of gravitating systems. These are fine for the inner parts. On the other hand, there has been much less work on DFs suitable for the radially anisotropic outer parts of the dark matter halos. In particular, a number of the suggestions in the literature for anisotropic DFs [e.g., 10, 11, 12, 13] are unsuitable, as they yield overwhelming radial anisotropy ($\beta \rightarrow 1$) in the outer parts, which is inconsistent with the simulations. While there exist some suggestions on the form of anisotropic DFs with a more flexible behavior of β [e.g., 14, 15], recovering such DFs for most density profiles is often analytically intractable [16, but see 17 for a special case].

II. DISTRIBUTION FUNCTIONS WITH $\beta = 1/2$

The widely used ansatz for a DF of a spherical system with constant anisotropy (parameterized by β) is

$$f(E, L) = L^{-2\beta} f_E(E) \quad (1)$$

where $E = \psi - v^2/2$ is the binding energy per unit mass, $L = rv_T$ is the specific angular momentum, and ψ is the relative potential. Integration of the DF over the velocity gives

$$\rho = r^{-2\beta} \frac{(2\pi)^{3/2} \Gamma(1-\beta)}{2^\beta \Gamma(3/2-\beta)} \int_0^\psi (\psi - E)^{1/2-\beta} f_E(E) dE. \quad (2)$$

The unknown function $f_E(E)$ then can be recovered from the integral inversion formula [13, 18];

$$f_E(E) = \frac{2^\beta (2\pi)^{-3/2}}{\Gamma(1-\lambda) \Gamma(1-\beta)} \frac{d}{dE} \int_0^E \frac{d\psi}{(E-\psi)^\lambda} \frac{d^n h}{d\psi^n} \quad (3)$$

where $h = r^{2\beta} \rho$ is expressed as a function of ψ , and $n = \lfloor (3/2 - \beta) \rfloor$ and $\lambda = 3/2 - \beta - n$ are the integer floor and the fractional part of $3/2 - \beta$. This includes Eddington’s formula [19] for the isotropic DF as a special case ($\beta = 0$). The expression for

*Electronic address: nwe@ast.cam.ac.uk

†Electronic address: jinan@space.mit.edu

the differential energy distribution (DED) reduces to [c.f., 13]

$$\frac{dM}{dE} = f_E(E) \frac{(2\pi)^{5/2} \Gamma(1-\beta)}{2^{\beta-1} \Gamma(3/2-\beta)} \int_0^{r_E} (\psi - E)^{1/2-\beta} r^{2(1-\beta)} dr. \quad (4)$$

Here, r_E is the radius of the largest orbit of a particle with energy E , that is to say, $\psi(r_E) = E$.

If β is a half-integer constant (i.e., $\beta = 1/2, -1/2$, and so on), the expression for DF further reduces to

$$f(E, L) = \frac{1}{2\pi^2} \frac{L^{-2\beta}}{(-2\beta)!!} \left. \frac{d^{3/2-\beta} h}{d\psi^{3/2-\beta}} \right|_{\psi=E}. \quad (5)$$

This involves only differentiations, as first noted by Cuddeford [13]. For the simplest case of $\beta = 1/2$, by utilizing the parameter r_E , the expressions for the DF and the DED can be simply written down as

$$\begin{aligned} f(E, L) &= \frac{g(r_E)}{2\pi^2 L}; \quad \frac{dM}{dE} = 2\pi r_E^2 g(r_E), \\ g(r_E) &= \left. \frac{\rho + r(d\rho/dr)}{(d\psi/dr)} \right|_{r=r_E} = \frac{\rho r_E^2}{GM_r} \left(-1 - \frac{d \ln \rho}{d \ln r} \right) \Big|_{r=r_E}, \end{aligned} \quad (6)$$

where M_r is the enclosed mass within the sphere of radius of r . So, the $\beta = 1/2$ case, which is desirable from the point of view of the N -body simulations, is also very attractive mathematically. That is, both the DF and DED can be found almost trivially from the potential-density pair.

III. COSMOLOGICAL HALO MODELS

A. Generalized NFW Profiles

Let us consider a family of centrally cusped density profiles

$$\rho = \frac{(b-2)\psi_0}{4\pi G} \frac{a^{b-2}}{r(r+a)^{b-1}} \quad (7)$$

where the parameter $b > 2$ is the asymptotic density power index at large radii, and ψ_0 is the depth of the central potential well. Near the center, the density for every member of this family is always cusped as r^{-1} . This reduces to the Hernquist [20] model for $b = 4$ whereas it becomes the ‘universal’ halo density law or so-called Navarro-Frenk-White (NFW) profile [7] if $b = 3$. The system has an infinite mass for $2 < b \leq 3$. On the other hand, if $b > 3$, the finite total mass is given by $GM_\infty = \psi_0 a / (b-3)$. The corresponding potential is

$$\psi = \frac{\psi_0 a}{r} \text{Ln}_{b-2} \left(\frac{r+a}{a} \right),$$

where, to reduce notational clutter, we have used the ‘ q -logarithm’ function [21] defined to be

$$\text{Ln}_q(x) \equiv \int_1^x \frac{dt}{t^q} = \begin{cases} (x^{1-q} - 1)/(1-q) & q \neq 1 \\ \ln x & q = 1 \end{cases}.$$

Here, we note also a property of q -logarithm function, namely $\text{Ln}_q(x^{-1}) = -\text{Ln}_{2-q}(x)$. Its inverse is the ‘ q -exponential’ function

$$\text{Ex}_q(x) = \text{Ln}_q^{-1}(x) = \begin{cases} [1 + (1-q)x]^{1/(1-q)} & q \neq 1 \\ \exp(x) & q = 1 \end{cases}.$$

The DF of the form of Eq. (1) can be found using (with $G = \psi_0 = a = 1$)

$$h = r^{2\beta} \rho = \frac{b-2}{4\pi} \frac{r^{2\beta-1}}{(1+r)^{b-1}}$$

and Eqs. (3) or (5). However, for $\beta = 1/2$, the formulas (6) enable us to write down the DF for all the family using r_E [here, $r_E E = \text{Ln}_{b-2}(1+r_E)$; see Appendix A for $b = 7/3, 5/2, 8/3, 7/2, 4$, or 5]. We find that

$$f(E, L) = \frac{b-2}{(2\pi)^3 L} \frac{(b-1)r_E}{(1+r_E)^b E - (1+r_E)^2}; \quad (8)$$

$$\frac{dM}{dE} = \frac{b-2}{2} \frac{(b-1)r_E^3}{(1+r_E)^b E - (1+r_E)^2}. \quad (9)$$

Here, E ranges in the interval $[0, 1]$ because $0 \leq E \leq \psi \leq 1$. Note that $r_E \rightarrow 0$ as $E \rightarrow 1$ and $r_E \rightarrow \infty$ as $E \rightarrow 0$. For all members of the family with $b > 2$, we find that the DF is non-negative for all accessible phase space volume. The behavior of the energy part of the DF (Eq. 8) and the DED (Eq. 9) of this family are shown in Fig. 1 for several values of b .

Lokas and Mamon [22] derived analytical expressions for various physical properties of the NFW profile including the profiles of the velocity dispersions and the kinetic and potential energy assuming isotropy, constant anisotropy, or an Osipkov[10, 11]-Merritt[12] type DF. However, they fell short of deriving any explicit DF with the exception of the isotropic DF, for which they gave the result of the numerical integration of the Eddington’s formula. In fact, (the numerical integrations of) the isotropic as well as the Osipkov-Merritt DFs and DEDs for the NFW profile have been investigated in detail by Widrow [23]. We nevertheless again note that the isotropic DF is suitable only for the very inner parts of dark matter halos and that the Osipkov-Merritt type DF is unsuitable in general, as it yields overwhelming radial anisotropy ($\beta \rightarrow 1$) in the outer parts.

It is relatively straightforward to find the asymptotic behavior of the DF and the DED near $E = 1$ by means of Taylor series expansion of r_E at $E = 1$. We find that $f(E = 1, L) = 2(b-1)/[(2\pi)^3 L]$ tends to a constant while $dM/dE \sim (1-E)^2 \rightarrow 0$ as $E \rightarrow 1$. On the other hand, the asymptotic behavior near $E = 0$ for $b \neq 3$ can be derived from $(3-b)r_E E \approx r_E^{3-b} - 1$ for $r_E \gg 1$. Then, we have

$$r_E \sim \begin{cases} E^{-1/(b-2)} & 2 < b < 3 \\ E^{-1} & b > 3 \end{cases},$$

for $0 \leq E \ll 1$. Consequently, the asymptotic forms of the DF and the DED are given by

$$f_E \sim \begin{cases} E^{1/(b-2)} & 2 < b < 3 \\ E^{b-2} & b > 3 \end{cases}; \quad \frac{dM}{dE} \sim \begin{cases} E^{-1/(b-2)} & 2 < b < 3 \\ E^{b-4} & b > 3 \end{cases}$$

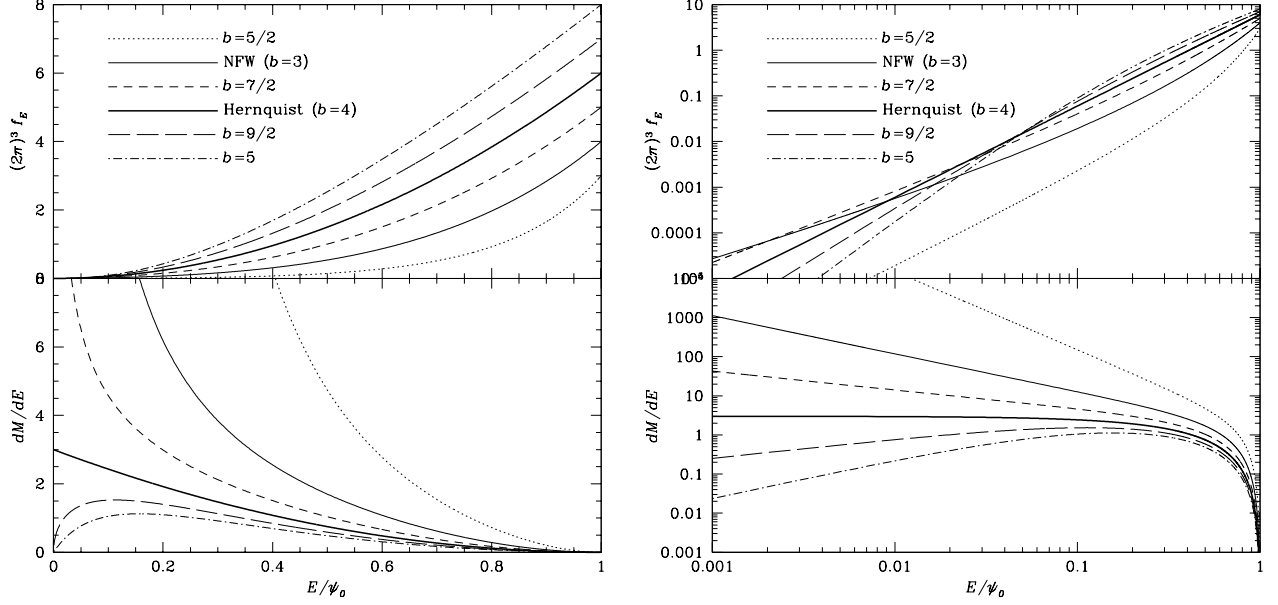


FIG. 1: The energy part of the distribution function (upper panel) and the differential energy distribution (lower panel) of the Navarro-Frenk-White family with the constant anisotropy parameter of $\beta = 1/2$: dotted lines ($b = 5/2$), thin solid lines ($b = 3$; NFW profile), short-dashed lines ($b = 7/2$), thick solid lines ($b = 4$; Hernquist model), long-dashed lines ($b = 9/2$), dot-dashed lines ($b = 5$). Note that the models are normalized to the common value of the depth of the central potential well, and, for $b \leq 3$, the total mass is divergent.

so that $f(E = 0, L) = 0$ whereas the DED diverges as $E \rightarrow 0$ if $b < 4$ and is finite otherwise. In particular, $\lim_{E \rightarrow 0} (dM/dE) = 0$ if $b > 4$, and $dM/dE|_{E=0} = 3$ if $b = 4$.

For the NFW profile ($b = 3$), the proper asymptotic form for the inversion of $E = r_E^{-1} \ln(1 + r_E)$ cannot be expressed using only elementary functions. Nevertheless, the continuous nature of the asymptotic behavior suggests that $dM/dE \sim E^{-1}$. In fact, since $E \sim r_E^{-1} \ln r_E$ and $dM/dE \sim r_E/(r_E E - 1) \sim r_E/\ln r_E$ as $r_E \rightarrow \infty$, this is indeed the right behavior for the NFW profile. We also note that it is possible to approximate as $r_E \sim E^{-1} \Omega(E)$ and $f_E \sim E[\Omega(E)]^{-2}$ where $\Omega(E) = -W_{-1}(-E) = \ln(E^{-1} \ln(E^{-1} \ln(E^{-1} \dots))) \approx \ln(E^{-1} \ln E^{-1})$. Here, $W_{-1}(x)$ is the real-valued second branch of Lambert W-function [24] such that $W_{-1}(x) < -1$ for $-e^{-1} < x < 0$. By comparison, we have $f \sim E^{3/2}[\Omega(E)]^{-3}$ and $dM/dE \sim E^{-1}$ for the same ($E \rightarrow 0$)-asymptotic behaviors of the isotropic DF and DED of the NFW profile [23].

As a brief illustration of the application of our DF (Eq. 8), we consider the direct detection of dark matter. Such experiments work by measuring the recoil energy of a nucleus in a low background laboratory detector that has undergone a collision with a dark matter particle. Although the deposited energy is tiny and the interactions are very rare, there are now many groups searching for this effect worldwide [e.g., 25, and references therein]. The detection rate depends on the masses m_χ and m_N of the dark matter particle and the target nucleus and the elastic scattering cross-section σ_0 between them. It also depends on the local dark matter density ρ_0 and the speed distribution of the dark matter particles (in the rest frame of the target).

The differential rate for detection per unit detector mass is given by [c.f., 26]

$$\frac{dR}{dE}\bigg|_{E=\mathcal{E}} = \frac{\sigma_0}{2m_\chi \mu^2} F^2(\mathcal{E}) \int \frac{d^3 \mathbf{v}}{|\mathbf{v}|} f(E, L) \Theta(|\mathbf{v}| - v_{\min}), \quad (10)$$

where $\Theta(x)$ is the Heaviside unit step function, \mathcal{E} is the recoil energy, $\mu^{-1} = m_N^{-1} + m_\chi^{-1}$ is the reduced mass, and

$$v_{\min} = \left(\frac{\mathcal{E} m_N}{2\mu^2} \right)^{1/2}.$$

In addition, $F(\mathcal{E})$ is the nuclear form factor, which is commonly modeled at least for scalar interaction by [27, 28]

$$F(\mathcal{E}) = \exp\left(-\frac{\mathcal{E}}{2\mathcal{E}_0}\right),$$

where \mathcal{E}_0 is the nuclear coherence energy. Here, the DF is normalized to the local density of the dark matter;

$$\rho_0 = \int d^3 \mathbf{v} f(E, L).$$

Note the integral in Eq. (10) is over the velocity with respect to the detector on Earth. Of course, the Earth revolves around the Sun while the Sun moves with respect to the Galactic inertial frame (in which the net angular momentum of the dark matter halo vanishes). This produces an annual modulation in the signal, which the experiments hope to detect.

The total event rate can be found by integrating over all detectable energies. For the sake of definiteness, we consider

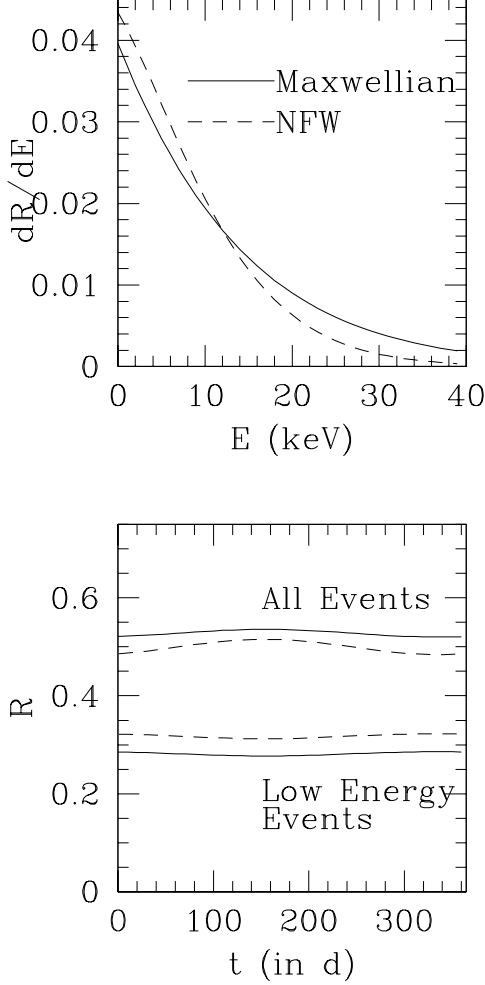


FIG. 2: Upper panel: The differential rate (in units of $\text{events kg}^{-1} \text{d}^{-1} \text{keV}^{-1}$) for the case of 40 GeV dark matter particles impinging on a cryogenic detector made of Ge. Results are shown for a standard isothermal sphere with Maxwellian DF (full line) and the NFW model with DF given by Eq. (8) (dashed line). Lower panel: The annual modulation signal (in units of $\text{events kg}^{-1} \text{d}^{-1}$) for the isothermal sphere and NFW models. The upper curves show the variation in the total rate, the lower curves the variation in the low energy events ($< 10 \text{ keV}$).

a dark matter particle with only scalar interactions and with a mass $m_\chi c^2 = 40 \text{ GeV}$ and cross-section $\sigma_0 = 4 \times 10^{-36} \text{ cm}^2$. The detector is made of ^{73}Ge . The local halo density is taken as $\rho_0 c^2 = 0.3 \text{ GeV cm}^{-3}$ [29].

We consider two models for the dark matter halo. The first is a standard isothermal sphere, with a flat rotation curve of amplitude $v_0 = 220 \text{ km s}^{-1}$. The DF is a Maxwell-Boltzmann distribution [5]. This is a useful benchmark, as the model is widely used in dark matter studies [e.g., 26]. The second is a NFW model (Eq. 7 with $b = 3$) with $a = 10 \text{ kpc}$, normalized to provide the assumed local halo density. The DF is given by Eq. (8).

The results for the differential rate and the annual modulation signal are shown in Fig. 2. The total rate is lower

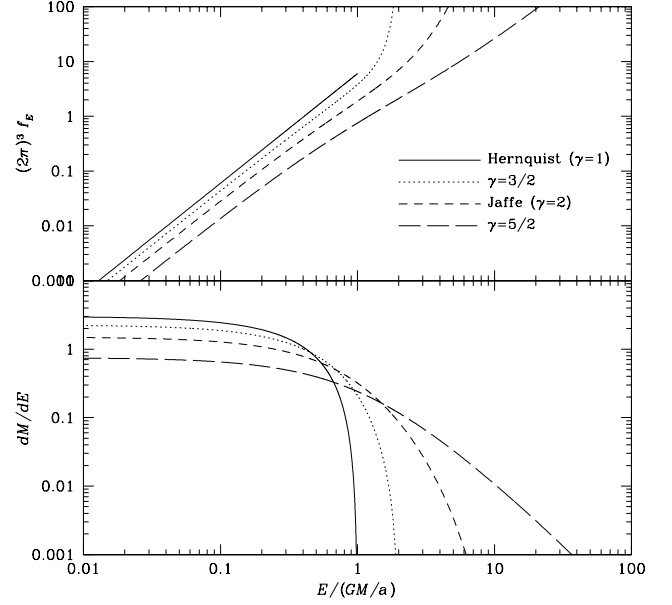


FIG. 3: The energy part of the distribution function (upper panel) and the differential energy distribution (lower panel) of the γ models with the constant anisotropy parameter of $\beta = 1/2$: solid lines ($\gamma = 1$; Hernquist model), dotted lines ($\gamma = 3/2$), short-dashed lines ($\gamma = 2$; Jaffe model), long-dashed lines ($\gamma = 5/2$). The models are normalized to the same total mass. For $\gamma \geq 2$, the central potential well depth is infinite so that E lies in the range $[0, \infty)$, whereas $0 \leq E \leq \psi_0 = (2 - \gamma)^{-1}(GM/a)$ for $\gamma < 2$.

by $\sim 10\%$ for the NFW model compared against the isothermal sphere. But, the peak-to-peak amplitude of the modulation signal has increased from $\sim 0.018 \text{ events kg}^{-1} \text{d}^{-1}$ to $\sim 0.030 \text{ events kg}^{-1} \text{d}^{-1}$. This renders the dark matter particle more detectable. However, this good news comes with a caveat. If the experiment is only sensitive to low energy events ($E < 10 \text{ keV}$) then the peak-to-peak variation in the modulation signal is actually smaller for the NFW model versus the standard isothermal sphere. The main differences between the two models is that the escape speed of dark matter particles is finite for the NFW model, but infinite for the isothermal sphere. Therefore, the former produces more low energy events, while the latter provides a larger total number of events.

B. The Gamma Spheres

As a second example of our formulas (6), we consider the potential-density pair of the γ model [30, 31]

$$\rho = \frac{(3 - \gamma)M}{4\pi} \frac{a}{r^\gamma(r + a)^{4-\gamma}}; \quad \psi = \frac{GM}{a} \text{Ln}_{3-\gamma} \left(\frac{r + a}{r} \right).$$

Here, the parameter $\gamma < 3$ is the three-dimensional central density slope (i.e., the central density is cusped as $r^{-\gamma}$ if $\gamma > 0$), and M is the total mass. At large radii, the density falls off as r^{-4} for every member of the family. The central potential well depth is infinite if $2 \leq \gamma < 3$, whereas, if $\gamma < 2$, the

potential is bounded as $0 \leq \psi \leq (2 - \gamma)^{-1}(GM/a)$. The family contains the Hernquist [20] model ($\gamma = 1$) and the Jaffe [32] model ($\gamma = 2$) as special cases.

If we define $y = r/(r + a)$, it is easy to write down ($G = M = a = 1$)

$$h = r^{2\beta} \rho = \frac{3 - \gamma}{4\pi} \frac{(1 - y)^{4-2\beta}}{y^{\gamma-2\beta}}.$$

Here, h can be written explicitly as a function of ψ using $y = \text{Ex}_{\gamma-1}(-\psi)$. Then, for $\beta = 1/2$, from Eq. (5), we find the DF and the DED,

$$f(E, L) = \frac{3 - \gamma}{(2\pi)^3 L} \frac{(1 - y_E)^2}{y_E} [(4 - \gamma)y_E + (\gamma - 1)] ; \quad (11)$$

$$\frac{dM}{dE} = \frac{3 - \gamma}{2} [(4 - \gamma)y_E + (\gamma - 1)] y_E \quad (12)$$

where $y_E = r_E/(1 + r_E) = \text{Ex}_{\gamma-1}(-E)$, which can be always expressible using elementary functions of E . Since $0 \leq y_E \leq 1$, the DF is everywhere non-negative only if $1 \leq \gamma < 3$ [33, c.f.,]. The behavior of the energy part of the DF (Eq. 11) and the DED (Eq. 12) of the γ models are shown in Fig. 3 for several values of γ .

As $E \rightarrow 0$ ($y_E \rightarrow 1$), we find that $f_E(E) \sim E^2 \rightarrow 0$ whereas the DED is always finite with the limiting value of $3(3 - \gamma)/2$. On the other hand, the asymptotic behavior as $E \rightarrow \psi_0$ ($y_E \rightarrow 0$), where $\psi_0 = \infty$ for $\gamma \geq 2$ or $\psi_0 = (2 - \gamma)^{-1}$ for $\gamma < 2$, are found to be $f_E \sim y_E^{-1}$ and $(dM/dE) \sim y_E$ where

$$y_E \sim \begin{cases} E^{-1/(\gamma-2)} & 2 < \gamma < 3 \\ e^{-E} & \gamma = 2 \\ (\psi_0 - E)^{1/(2-\gamma)} & 1 < \gamma < 2 \end{cases},$$

except for the limiting case of $\gamma = 1$ (the Hernquist model), for which $f(E, L) = 3(4\pi^3)^{-1} L^{-1} (1 - y_E)^2 = 3(4\pi^3)^{-1} E^2 L^{-1}$ and $(dM/dE) = 3y_E = 3(1 - E)^2$. Note that the asymptotic behavior of the DED at both limits are the same as those for the isotropic DF [30] for $1 < \gamma < 3$ despite the fact that the behavior of the DFs are rather distinct.

IV. THE UNIVERSAL ASYMPTOTIC BEHAVIOR

The asymptotic behaviors derived for the DF and DED in the preceding sections strongly suggest that they are simply determined by the anisotropy parameter and the density power index at the center and at the infinity. Even more interestingly, the DED appears to be completely determined (up to scale) by the density power index alone. Assuming that this is indeed the case, we predict asymptotic behaviors of generic DFs and DEDs by generalizing the method of Hjorth and Madsen [34], while allowing for anisotropy by means of the ansatz (1).

First, the self-consistent potential due to the asymptotic density profile of $\rho \sim r^{-\alpha}$ is

$$\psi \sim \begin{cases} r^{-1} & \alpha > 3 \\ r^{-(\alpha-2)} & 2 < \alpha < 3 \end{cases},$$

$$(\psi_0 - \psi) \sim r^{2-\alpha} \quad \alpha < 2$$

Here, since the case that $\alpha > 3$ is only allowed for the asymptotic falloff at infinity, the potential should tend to the Keplerian finite mass limit. Next, if we assume f_E to be roughly scale-free with $f_E \sim E^n$ (for $\alpha > 2$) or $f_E \sim (\psi_0 - E)^n$ (for $\alpha < 2$), we find from Eq. (2)

$$\rho \sim \begin{cases} r^{-2\beta} \psi^{n-\beta+3/2} & \alpha > 2 \\ r^{-2\beta} (\psi_0 - \psi)^{n-\beta+3/2} & \alpha < 2 \end{cases}.$$

In order for this to be $\rho \sim r^{-\alpha}$ with the self-consistent potential, we should have

$$L^{2\beta} f(E, L) \sim \begin{cases} E^{\alpha-\beta-(3/2)} & \alpha > 3 \\ E^{\beta-(1/2)+p} & 2 < \alpha < 3 \\ \exp[2(1-\beta)E] & \alpha = 2 \\ (\psi_0 - E)^{\beta-(1/2)-(-p)} & 2\beta < \alpha < 2 \end{cases} \quad (13)$$

where $p = 2(1 - \beta)/(\alpha - 2)$. Here, α and β are the limiting values at the center (for behavior near $E \sim \psi_0$) or the asymptotic value toward infinity (for behavior near $E \sim 0$). As for the DED, by changing the integration variable to ψ/E (for $\alpha > 2$) or $(\psi_0 - \psi)/(\psi_0 - E)$ (for $\alpha < 2$) in Eq. (4), and combined with Eqs. (13), we find that,

$$\frac{dM}{dE} \sim \begin{cases} E^{\alpha-4} & \alpha > 3 \\ E^{-1/(\alpha-2)} & 2 < \alpha < 3 \\ \exp(-E) & \alpha = 2 \\ (\psi_0 - E)^{1/(2-\alpha)} & 2\beta < \alpha < 2 \end{cases}. \quad (14)$$

It is independent of the anisotropy. We note that the coefficient for the leading order term of f_E changes its sign at $\alpha = 2\beta$ so that the result is invalid at the limit $\alpha = 2\beta$ and that the DF is unphysical for $\alpha < 2\beta$ [33].

Here, since $\alpha < 3$ at the center, $\lim_{E \rightarrow \psi_0} dM/dE = 0$ (where $\psi_0 = \infty$ if $2 \leq \alpha < 3$) for all physical values of α . On the other hand, the behavior of dM/dE near $E = 0$ for a finite mass system (i.e., $\alpha > 3$) implies that dM/dE diverges for $\alpha < 4$ while it is finite for $\alpha \geq 4$ (in particular, $dM/dE \rightarrow 0$ if $\alpha > 4$). It has been argued before that violent relaxation produces an r^{-4} density falloff at large radii [6]. This may be inferred from the generic behavior of dM/dE at the asymptotic limit $E \rightarrow 0$ (note that the behavior of dM/dE near $E = 0$ is dominated by the particles at large radii). That is, the loss of loosely bound particles at large radii due to velocity perturbations is much more significant if the initial density falloff is shallower than r^{-4} while it becomes rather insignificant once the density falloff gets steeper than r^{-4} . Therefore, any perturbation drives systems with initially shallower density falloff to settle toward the r^{-4} falloff or a slightly steeper slope. Note that this argument is completely independent of the anisotropy since the asymptotic form of dM/dE is also independent of β .

If one considers the case that the gravitational field is dominated not by the self-consistent potential but by the Keplerian field due to the central black hole, it is straightforward to see that the same argument leads to the asymptotic behavior of $f_E \sim E^{\alpha-\beta-3/2}$ and $dM/dE \sim E^{\alpha-4}$ for all allowed values of $\alpha > \beta + 1/2$ except also for the limiting case $\alpha = \beta + 1/2$, for which the otherwise leading term identically vanishes.

V. CONCLUSIONS

Except close to the very center, dark matter halos have distribution functions (DFs) that are radially anisotropic with an anisotropy parameter $\beta \approx 0.5$. Constant anisotropy distribution functions with $\beta = 1/2$ are very simple to construct – far simpler than Eddington’s awkward Abel transformation pair for the isotropic model. This paper provides simple inversion formulas (6), which enables such DFs and the corresponding differential energy distributions to be built for any spherical model, provided that its potential and density are known.

We have also given the *generic* form of the DF for any spherical model with a local density power index α ($\rho \sim r^{-\alpha}$) and anisotropy parameter β . In the central parts of simulated halos where $\alpha \approx 1$ and $\beta \approx 0$, we find $f(E) \sim (\psi_0 - E)^{-5/2}$ and $dM/dE \sim (\psi_0 - E)$. In the envelopes of simulated halos with $\beta \approx 1/2$, we have DFs, which range from

$$f(E, L) \sim \frac{1}{L} \frac{E}{\Lambda(E)}; \quad \frac{dM}{dE} \sim \frac{1}{E}$$

if $\alpha \approx 3$ [where $\Lambda(E)$ is some function that diverges or vanishes no faster than finite power of the logarithm as $E \rightarrow 0$],

to

$$f(E, L) \sim \frac{E^2}{L}; \quad \frac{dM}{dE} \sim E^0$$

if $\alpha \approx 4$. Finally, we have argued that falloff of the density at large radii must have evolved to $\rho \sim r^{-4}$ or steeper in the long run. This argument is independent of the velocity anisotropy.

Using our DF for the NFW profile, we calculated the direct detection rate for a cosmological halo model with a radially anisotropic DF. We showed that the annual modulation signal is larger in radially anisotropic ($\beta = 1/2$) cosmological halo models than in isotropic isothermal spheres. This may be welcome good news for dark matter experimentalists.

APPENDIX A

If $b = 7/3, 5/2, 8/3, 7/2, 4$, or 5 , then the integral of motion r_E for the generalized NFW profiles is expressible analytically in terms of the energy by solving a quadratic or linear equation, viz ($G = \psi_0 = a = 1$)

$$\begin{aligned} r_E &= \frac{4(1-E)}{E^2} & \text{for } b = \frac{5}{2}; & & r_E &= \frac{1-E}{E} & \text{for } b = 4; \\ r_E &= \frac{9(3-4E^2) + 3^{3/2}(3-2E)^{3/2}\sqrt{1+2E}}{16E^3} & \text{for } b = \frac{7}{3}; & & r_E &= \frac{3^{3/2}\sqrt{4-E}}{2E^{3/2}} - \frac{9}{2E} & \text{for } b = \frac{8}{3}; \\ r_E &= \frac{4-E-E^{1/2}\sqrt{8+E}}{2E} & \text{for } b = \frac{7}{2}; & & r_E &= \frac{1-4E+\sqrt{1+8E}}{4E} & \text{for } b = 5. \end{aligned}$$

For all other values of b , the function $r_E(E)$ is straightforward to construct numerically.

-
- [1] J. E. Taylor and J. F. Navarro, *Astrophys. J.* **563**, 483 (2001), astro-ph/0104002.
 - [2] S. H. Hansen, B. Moore, and J. Stadel, arXiv *Astrophys. e-prints* (2005), astro-ph/0509799.
 - [3] S. H. Hansen and B. Moore, *New Astron.* **11**, 333 (2006), astro-ph/0411473.
 - [4] S. H. Hansen and J. Stadel, arXiv *Astrophys. e-prints* (2005), astro-ph/0510656.
 - [5] J. Binney and S. Tremaine, *Galactic dynamics* (Princeton Univ. Press, Princeton NJ, 1987).
 - [6] W. Jaffe, in *Structure and Dynamics of Elliptical Galaxies*, edited by P. T. de Zeeuw (D. Reidel, Dordrecht, 1987), no. 127 in IAU Symp., pp. 511–512.
 - [7] J. F. Navarro, C. S. Frenk, and S. D. M. White, *Mon. Not. R. Astron. Soc.* **275**, 720 (1995), astro-ph/9408069.
 - [8] D. Lynden-Bell, *Mon. Not. R. Astron. Soc.* **136**, 101 (1967).
 - [9] R. P. van der Marel, *Mon. Not. R. Astron. Soc.* **270**, 271 (1994).
 - [10] L. P. Osipkov, *Pis'ma Astron. Zh.* **5**, 77 (1979).
 - [11] L. P. Osipkov, *Soviet Astron. Lett.* **5**, 42 (1979).
 - [12] D. Merritt, *Astron. J.* **90**, 1027 (1985).
 - [13] P. Cuddeford, *Mon. Not. R. Astron. Soc.* **253**, 414 (1991).
 - [14] O. E. Gerhard, *Mon. Not. R. Astron. Soc.* **250**, 812 (1991).
 - [15] P. D. Louis, *Mon. Not. R. Astron. Soc.* **261**, 283 (1993).
 - [16] P. Cuddeford and P. Louis, *Mon. Not. R. Astron. Soc.* **275**, 1017 (1995).
 - [17] H. Dejonghe, *Mon. Not. R. Astron. Soc.* **224**, 13 (1987).
 - [18] J. H. An and N. W. Evans, *Astron. J.* **131**, in press (2006), astro-ph/0501092.
 - [19] A. S. Eddington, *Mon. Not. R. Astron. Soc.* **76**, 572 (1916).
 - [20] L. Hernquist, *Astrophys. J.* **356**, 359 (1990).
 - [21] C. Tsallis, *J. Statistical Phys.* **52**, 479 (1988).
 - [22] E. L. Łokas and G. A. Mamon, *Mon. Not. R. Astron. Soc.* **321**, 155 (2001), astro-ph/0002395.
 - [23] L. M. Widrow, *Astrophys. J. Suppl. Ser.* **131**, 39 (2000).
 - [24] R. M. Corless, G. H. Gonnet, D. E. G. Hare, D. J. Jefferey, and D. E. Knuth, *Advances Comput. Math.* **5**, 329 (1996).
 - [25] *The Identification of Dark Matter, Proceedings of the Fifth International Workshop*, edited by N. J. C. Spooner and V. Kudryavtsev (World Scientific, Singapore, 2005).
 - [26] G. Jungman, M. Kamionkowski, and K. Griest, *Phys. Rep.* **267**, 195 (1996), hep-ph/9506380.
 - [27] S. P. Ahlen, F. T. Avignone, R. L. Brodzinski, A. K. Drukier, G. Gelmini, and D. N. Spergel, *Phys. Lett. B* **195**, 603 (1987).
 - [28] K. Freese, J. Frieman, and A. Gould, *Phys. Rev. D* **37**, 3388 (1988).
 - [29] E. I. Gates, G. Gyuk, and M. S. Turner, *Astrophys. J.* **449**, L123 (1995), astro-ph/9505039.
 - [30] W. Dehnen, *Mon. Not. R. Astron. Soc.* **265**, 250 (1993).
 - [31] S. Tremaine, D. O. Richstone, Y.-I. Byun, A. Dressler, S. M. Faber, C. Grillmair, J. Kormendy, and T. R. Lauer, *Astron. J.* **107**, 634 (1994), astro-ph/9309044.
 - [32] W. Jaffe, *Mon. Not. R. Astron. Soc.* **202**, 995 (1983).
 - [33] J. H. An and N. W. Evans, *Astrophys. J.* **000**, in press (2006), astro-ph/0511686.
 - [34] J. Hjorth and J. Madsen, *Mon. Not. R. Astron. Soc.* **253**, 703 (1991).